# Parametric study of noise reduction by an air-bubble curtain in offshore pile driving

Tsouvalas, Apostolos; Metrikine, Andrei V.

**Publication date**
2016

**Published in**
ICSV 2016 - 23rd International Congress on Sound and Vibration: From Ancient to Modern Acoustics

**Citation (APA)**
Tsouvalas, A., & Metrikine, A. V. (2016). Parametric study of noise reduction by an air-bubble curtain in offshore pile driving. In *ICSV 2016 - 23rd International Congress on Sound and Vibration: From Ancient to Modern Acoustics* (pp. 1-8). Article 123390 International Institute of Acoustics and Vibrations.

23rd International Congress on Sound & Vibration
Athens, Greece 10-14 July 2016
ICSV23

# PARAMETRIC STUDY OF NOISE REDUCTION BY AN AIR-BUBBLE CURTAIN IN OFFSHORE PILE DRIVING

Apostolos Tsouvalas
*Delft University of Technology, Faculty of Civil Engineering and Geosciences, Section of Offshore Engineering, Stevinweg 1, Delft, The Netherlands*
*email: a.tsouvalas@tudelft.nl*

Andrei V. Metrikine
*Delft University of Technology, Faculty of Civil Engineering and Geosciences, Section of Structural Mechanics, Stevinweg 1, Delft, The Netherlands*

This paper describes a semi-analytical model that is used for the investigation of the sound reduction during marine piling when an air-bubble curtain is placed around the pile. The model consists of the pile, the surrounding water and soil media, and the air-bubble curtain which is positioned at a certain distance from the pile surface. The aim of the paper is to analyse the principal mechanisms that are responsible for the noise reduction due to the application of the air-bubble curtain in marine piling. The results show that the noise reduction depends strongly on the frequency content of the radiated sound and on the characteristics of the bubbly medium. For piles of large diameter, which are typically used nowadays as foundation piles for offshore wind power generators, the noise reduction is mainly attributed to the reflection of the acoustic waves at the inner surface between the seawater and the bubbly layer. On the contrary, for piles of smaller diameter and when the radiated acoustic energy is concentrated at frequencies closer to, or higher than, the first omnidirectional resonance frequency of the air bubbles, the sound absorption within the bubbly layer and its thickness become critical.

## 1. Introduction

Noise pollution in the sea environment is often a by-product of marine industrial operations. The problem has gained considerable attention in the recent years mainly due to the large number of offshore wind farms under construction. Nowadays, large-size steel piles are used as foundations of the offshore wind power generators which are driven into the sediment with the help of impact hammers [1]. The installation generates high noise levels in the seawater region which can be harmful for the marine species [2, 3, 4]. Since the reduction of the underwater noise is a key issue in the anti-noise legislation imposed by different nations [5], several noise mitigation concepts have been developed [6]. Among the various solutions proposed, the air-bubble curtain is usually chosen due to its long-standing history and simple configuration. An air-bubble curtain consists of rising air bubbles that encircle the pile forming thus a *closed curtain* of certain thickness [7]; the freely rising bubbles are created by compressed air that is injected through perforated pipes positioned either horizontally on the seabed level or vertically fixed at a framed structure [8]. Despite the plethora of the available bubble-curtain configurations that have been developed, all of them share the same basic principle of noise reduction.

In a series of previous publications by the authors, a number of models have been developed that allowed an in-depth investigation of the generation mechanisms and the propagation characteristics

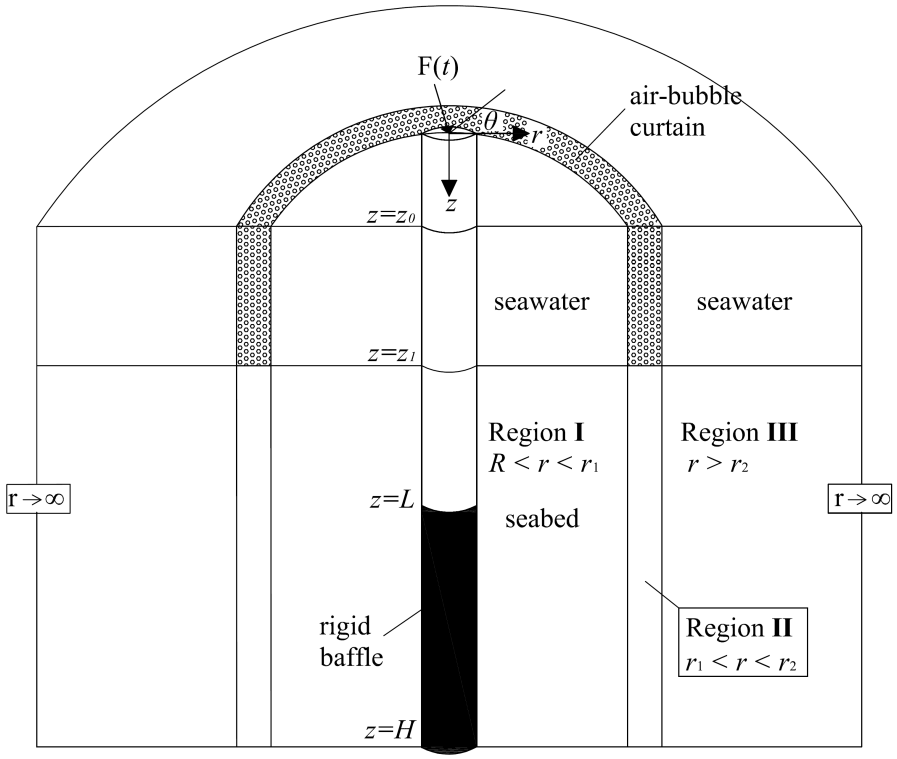


Figure 1: Geometry of the model with the air-bubble curtain surrounding the pile at a distance $r = r_1$. The thickness of the air-bubble curtain is $t = r_2 - r_1$. The tip of the pile is located at $z = L$ and the remaining part is substituted by a rigid baffle.

of the underwater sound during marine piling [9, 10]. In this paper, a three-dimensional model is presented that includes additionally the air-bubble curtain. The solution approach is based on the dynamic sub-structuring technique and the modal decomposition method. This method is similar to the one presented in [10] but is generalised here to account for the inhomogeneity along the horizontal direction introduced by the presence of the air-bubble curtain. In addition, the focus is placed on the noise reduction due to the application of the air-bubble curtain. The seabed is described as a linearised fluid with extra attenuation to account for the energy transferred into shear waves in the soil domain.

The developed model is used to perform a parametric study in order to reveal the principal mechanisms that are responsible for the noise reduction for different system configurations. The influence of the size of the air bubbles, the volume of the air content, and the thickness of the bubble curtain on the predicted sound levels are investigated. The paper is structured as follows. In section 2, the semi-analytical model is introduced together with the governing equations and the solution method. In addition, the background theory used to model the dynamic behaviour of the air-water mixture is briefly presented. A detailed derivation of the mathematical expressions can be found in a recent paper by the authors [11]. In section 3, a parametric study is performed and the generated wave field is analysed for the case of a large-size pile (section 3.1) and the case of a small-size pile (section 3.2). Finally, section 4 gives an overview of the results of this study together with some points that require further investigation.

## 2. Description of the model

The geometry of the model is shown schematically in Fig.1. It consists of four sub-domains corresponding to the pile and the three external regions. The pile is modelled as a thin elastic cylindrical shell [12]. The constants $E, \nu, \rho, 2h$ and $R$ correspond to the complex-valued modulus of elasticity, Poisson's ratio, density, thickness and radius of the mid-surface of the shell, respectively. The pile is

surrounded by fluid at $z_0 < z < z_1$ and by soil at $z_1 < z < L$. The soil occupies the region $z \geq z_1$ and is terminated at a large depth ($z = H$) with a rigid boundary. The sea surface is positioned at $z = z_0$ and is modelled as a pressure release boundary. The hammer is substituted by an external force applied at the top of the shell.

The exterior to the pile domain is divided into three regions as explained hereafter. Region **I** is bounded by $R \leq r \leq r_1$ and $z_0 \leq z \leq H$. It consists of the water column with a wave speed of $c_w$ and a density of $\rho_w$, overlying a layered soil medium. The latter is modelled an acoustic medium [13]. The shear rigidity of the seabed is neglected and the energy transferred to shear waves is accounted for by an extra attenuation in the region $z_1 \leq z \leq H$ included in the compressional wave speed. The friction of the soil along the pile shaft is accounted for by distributed shear springs positioned along the embedded length of the pile into the soil [9]. Region **II** occupies the domain $r_1 \leq r \leq r_2$ and $z_0 \leq z \leq H$. It consists of an air-bubble curtain (mixture of water and air bubbles) from $z_0 \leq z \leq z_1$ overlying a layered soil medium. The air-bubble curtain is modelled as a homogeneous fluid layer with modified compressibility and density to account for the presence of the air-bubbles. The estimation of the effective compressibility, wave speed, density and attenuation coefficient for the air-bubble curtain is based on the studies by Novarini et al. [14] and Hall [15]. For a detailed discussion of the theoretical modelling of the air-bubble curtain and the justification of the various choices the reader is referred to [11]. Region **III** consists of the water column with properties $c_w$, $\rho_w$ and the layered soil, both of which extend to infinity in the radial direction. The governing equations describing the vibroacoustic behaviour are:

$$\mathbf{L}\mathbf{u}_p + \mathbf{I}\mathbf{u}_p = -H(z-z_1)\mathbf{K}_s\mathbf{u}_p - H(z-z_0)\mathbf{p}^I + \mathbf{f}_e\,, 0 \leq z \leq L\,,\, r = R \tag{1}$$

$$\nabla^2\phi^j(r,\theta,z,t) - \frac{1}{c_j^2(z)}\frac{\partial^2\phi^j(r,\theta,z,t)}{\partial t^2} = 0\,,\; z_0 \leq z \leq H\,,\; R \leq r \leq r_1\,,\; j = \text{I,II,III} \tag{2}$$

$$v_r^I(R,\theta,z,t) = \frac{\partial u_{p,r}(z,\theta,t)}{\partial t}\,,\; z_0 < z < L \tag{3}$$

$$v_r^I(r_1,\theta,z,t) = v_r^{II}(r_1,\theta,z,t)\;,\; p^I(r_1,\theta,z,t) = p^{II}(r_1,\theta,z,t)\,,\; z_0 < z < H \tag{4}$$

$$v_r^{II}(r_2,\theta,z,t) = v_r^{III}(r_2,\theta,z,t)\;,\; p^{II}(r_2,\theta,z,t) = p^{III}(r_2,\theta,z,t)\,,\; z_0 < z < H \tag{5}$$

In Eq.(1), $\mathbf{u}_p = [u_{p,z}(z,\theta,t) \quad u_{p,\theta}(z,\theta,t) \quad u_{p,r}(z,\theta,t)]^{\mathrm{T}}$ is the displacement vector of the mid-surface of the shell. The operators $\mathbf{L}$ and $\mathbf{I}$ are the stiffness and inertia matrices of the shell given in [10]. The operator $\mathbf{K}_s$ accounts for the soil dynamic stiffness and is given in [9] with the exemption that the radial component is set equal to zero due to the fact that the reaction of the soil in the radial direction is accounted for explicitly here by the fluid description of the seabed. The sound speed in each region is $z-$dependent due to the difference in the phase velocities of the compressional waves in the water and in the soil. In addition to the equations above, the following conditions are imposed within each region: (i) pressure release boundary at $z = z_0$; (ii) continuity of vertical velocities and pressures at each horizontal interface between the various fluid layers; and (iii) vertical particle velocity equal to zero at $z = H$. Finally, the condition of finite response at infinite distance from the source and the radiation condition at $r \to \infty$ are considered for region III.

To obtain the solution to the coupled vibroacoustic system, equations (1)-(5) are first transformed to the frequency domain. The vertical eigenshapes in each subregion are then obtained by solving an eigenvalue problem which is independent of the circumferential-radial dependence of the field and inherently satisfies conditions (i)-(iii) described above. The result of this procedure is a set of eigenvalues and eigenmodes at each of the three regions. The pressure in the frequency domain at

each region can be expressed as:

$$\tilde{p}^I(r,\theta,z,\omega) = \sum_{n=0}^{\infty}\sum_{p=1}^{\infty}\left(A_{np}^{+}\,J_n(k_p^I\,r) + A_{np}^{-}\,Y_n(k_p^I\,r)\right)\,\tilde{p}_p^I(z,\omega)\,\cos(n\theta) \tag{6}$$

$$\tilde{p}^{II}(r,\theta,z,\omega) = \sum_{n=0}^{\infty}\sum_{q=1}^{\infty}\left(B_{nq}^{+}\,J_n(k_q^{II}\,r) + B_{nq}^{-}\,Y_n(k_q^{II}\,r)\right)\,\tilde{p}_q^{II}(z,\omega)\,\cos(n\theta) \tag{7}$$

$$\tilde{p}^{III}(r,\theta,z,\omega) = \sum_{n=0}^{\infty}\sum_{l=1}^{\infty}C_{nl}^{+}\,H_n^2(k_l^{III}\,r)\,\tilde{p}_l^{III}(z,\omega)\,\cos(n\theta) \tag{8}$$

Similar expressions hold for the velocity components in the radial and vertical directions [11] but are omitted here for the sake of brevity. The wavenumbers $k_p^I$, $k_q^{II}$ and $k_l^{III}$ are obtained by solving a separate eigenvalue problem for regions I, II and III, respectively. The coefficients $A_{np}^{+}$ and $A_{np}^{-}$ denote the amplitude of mode $(n,p)$ multiplied by the corresponding Bessel functions; the coefficients $B_{nq}^{+}$ and $B_{nq}^{-}$ are defined in a similar way. In region III only a transmitted wave field exists and therefore the coefficients $C_{nl}^{-}$ are omitted altogether while the Hankel functions of the proper kind are considered under the modal summation. The shell response is expressed in the modal domain as [9]:

$$u_j(z,\theta,t) = \sum_{n=0}^{\infty}\sum_{m=1}^{\infty}D_{nm}\,u_{jnm}(z,\theta,t) \tag{9}$$

As can be seen, the only unknowns in Eqs.(6)-(9) are the complex-valued coefficients for the fluid region, i.e. $A_{np}^{+}$, $A_{np}^{-}$, $B_{nq}^{+}$, $B_{nq}^{-}$, $C_{nl}^{+}$, and the modal coefficients of the shell structure $D_{nm}$. These coefficients can be obtained by satisfying the kinematic and dynamic conditions as given by Eqs.(3)-(5) together with Eq.(1).

To solve the coupled problem, Eqs.(1) and (3)-(5) are first transformed to the frequency domain. The satisfaction of stress equilibrium and displacement continuity along the various vertical interfaces together with the consideration of the forced equations of motion of the shell structure yields the following set of coupled algebraic equations [11]:

$$\begin{aligned}&\sum_{p=1}^{P}A_{np}^{+}\left(\Gamma_p\,J_n'(k_p^I\,R)\delta_{pk} - \sum_{m=1}^{M}\frac{J_n(k_p^I\,R)\,R_{nmp}\,R_{nmk}}{L_{nm}}\right) + \\ &\sum_{p=1}^{P}A_{np}^{-}\left(\Gamma_p\,Y_n'(k_p^I\,R)\delta_{pk} - \sum_{m=1}^{M}\frac{Y_n(k_p^I\,R)\,R_{nmp}\,R_{nmk}}{L_{nm}}\right) = \sum_{m=1}^{M}\frac{F_{nm}\,R_{nmk}}{L_{nm}}\end{aligned} \tag{10}$$

$$\left[A_{np}^{+}\,J_n'(k_p^I\,r_1) + A_{np}^{-}\,Y_n'(k_p^I\,r_1)\right]\Gamma_p = \sum_{q=1}^{Q}\left[B_{nq}^{+}\,J_n'(k_q^{II}\,r_1) + B_{nq}^{-}\,Y_n'(k_q^{II}\,r_1)\right]S_{qp}^{I-II} \tag{11}$$

$$\sum_{p=1}^{P}\left[A_{np}^{+}\,J_n(k_p^I\,r_1) + A_{np}^{-}\,Y_n(k_p^I\,r_1)\right]S_{qp}^{I-II} = \left[B_{nq}^{+}\,J_n(k_q^{II}\,r_1) + B_{nq}^{-}\,Y_n(k_q^{II}\,r_1)\right]\Delta_q \tag{12}$$

$$\begin{aligned}&\sum_{q=1}^{Q}B_{nq}^{+}\left(J_n'(k_q^{II}\,r_2)\Delta_q\delta_{jq} - \sum_{l=1}^{L}H_n'^2(k_l^{III}\,r_2)\,S_{lq}^{II-III}\,\frac{J_n(k_q^{II}\,r_2)S_{lj}^{II-III}}{H_n^2(k_l^{III}\,r_2)\,\Gamma_l}\right) + \\ &+\sum_{q=1}^{Q}B_{nq}^{-}\left(Y_n'(k_q^{II}\,r_2)\Delta_q\delta_{jq} - \sum_{l=1}^{L}H_n'^2(k_l^{III}\,r_2)\,S_{lq}^{II-III}\,\frac{Y_n(k_q^{II}\,r_2)S_{lj}^{II-III}}{H_n^2(k_l^{III}\,r_2)\,\Gamma_l}\right) = 0\end{aligned} \tag{13}$$

The integration constants $\Gamma_{p;l}$, $R_{nmp}$, $R_{nmk}$, $L_{nm}$, $F_{nm}$, $S_{qp}^{I-II}$ and $S_{lq}^{II-III}$ introduced in Eqs.(10)-(13) are given in [11] and are omitted here for the sake of brevity. The infinite summations need

to be truncated, i.e. the upper limits $P$ and $Q$ of the summations need to be properly chosen. A straightforward manner of truncation of the modal summations is generally unknown but rules of convergence of the pressure and velocity fields at the various interfaces can be applied similarly to [16].

## 3. Parametric Study

In this section, a parametric study is conducted in order to investigate the critical parameters of the system that determine largely the noise reduction potential of an air-bubble curtain (ABC). The sound radiation is investigated for two cases, i.e. a large-diameter pile (section 3.1) and a small-diameter pile (section 3.2).

### 3.1 Piles of large diameter

The sound radiation during the installation of a large pile is examined with and without the use of an air-bubble curtain. The pile properties are given as: $E = 210$GPa, $\nu = 0.28$, $\rho = 7850\text{kgm}^{-3}$, $\eta_p = 0.001$, $R = 2.7$m, $L = 58$m, and $2h = 50$mm. In accordance with Fig.1, the following coordinates are defined: $z_0 = 5$m, $z_1 = 23$m and $H = 90$m. The waveguide chosen consists of a seawater column with a depth of $18$m overlying a water-saturated fine sand medium with a thickness of $67$m. The density of the seawater region equals $1023\text{kgm}^{-3}$ and the sound speed $1453\text{ms}^{-1}$. The density of the seabed equals $1900\text{kgm}^{-3}$ and the sound speed $1797\text{ms}^{-1}$. An extra dissipation is added to the compressional wave speed in the seabed region to account for the energy the is lost into shear waves which is equal to $k_p = 0.4$ dB(m kHz)$^{-1}$ [17]. The bubble curtain is positioned at $r = 10$m and has a thickness of $1$m. It is assumed that the air bubbles are of approximately equal size and are uniformly distributed in the volume of the air-water mixture. The air-volume fraction and the bubble radius are $0.5\%$ and $1$mm, respectively. With these properties the air-bubble layer has an effective density of $\rho_e = 1018\text{kgm}^{-3}$ and an average phase velocity at the region $0 - 800$Hz (the medium is only slightly dispersive at this frequency range) of about $\text{Re}(c_e) = 226\text{ms}^{-1}$. The force exerted by the impact hammer is totally vertical, has an impulsive character with a pulse duration of $0.005$s and a peak amplitude of about $120$MN.

The generated sound fields are shown in Fig.2 for different moments in time after the impact. The pressure field is plotted against the radial and vertical coordinates at each time moment. Due to the verticality of the force no variation of the field exists along the circumferential coordinate. As can be seen, the pressure fields with and without the ABC are identical for $t \leq 12$ms due to the fact that the wave fronts have not yet reached the position of the bubble curtain. At $t = 14.4$ms, the first wave front reaches the inner side of the bubble curtain and part of the energy is reflected backwards into the domain formed by the outer surface of the pile and the inner side of the bubble curtain. Another part of the energy is transmitted through the bubble curtain.

The air-volume fraction is known to be a critical parameter in the determination of the sound speed and attenuation in the bubbly medium. Four cases are investigated which differ only by the percentile ratio of the air volume in the bubbly medium; the air-volume fraction is varied from $0.1\%$ to $2\%$. The average wave speed for frequencies up to $800$Hz varies from $482$ ms$^{-1}$ ($V_a = 0.1\%$) to $115$ ms$^{-1}$ ($V_a = 2\%$). The difference in the SPL ($\Delta$SPL) and the SEL ($\Delta$SEL)with and without the ABC is plotted versus the (i) air-volume fraction and (ii) the ratio of the acoustic impedances $\text{Re}(\tilde{c}_e)\,\rho_e/c_w\,\rho_w$ in Fig.3. As can be seen, the overall reduction of the pressure levels is not proportional to the increase in the percentile ratio of the air-volume in the mixture. An increase in the impedance contrast between the seawater and the bubbly medium yields an increased efficiency of the air-bubble curtain in terms of noise reduction. It is also important to mention that for large volumes of air in the bubbly medium, the interaction between the individual bubbles becomes important; a phenomenon which cannot be described by the adopted theory. Other parameters were also investigated but they found to be less

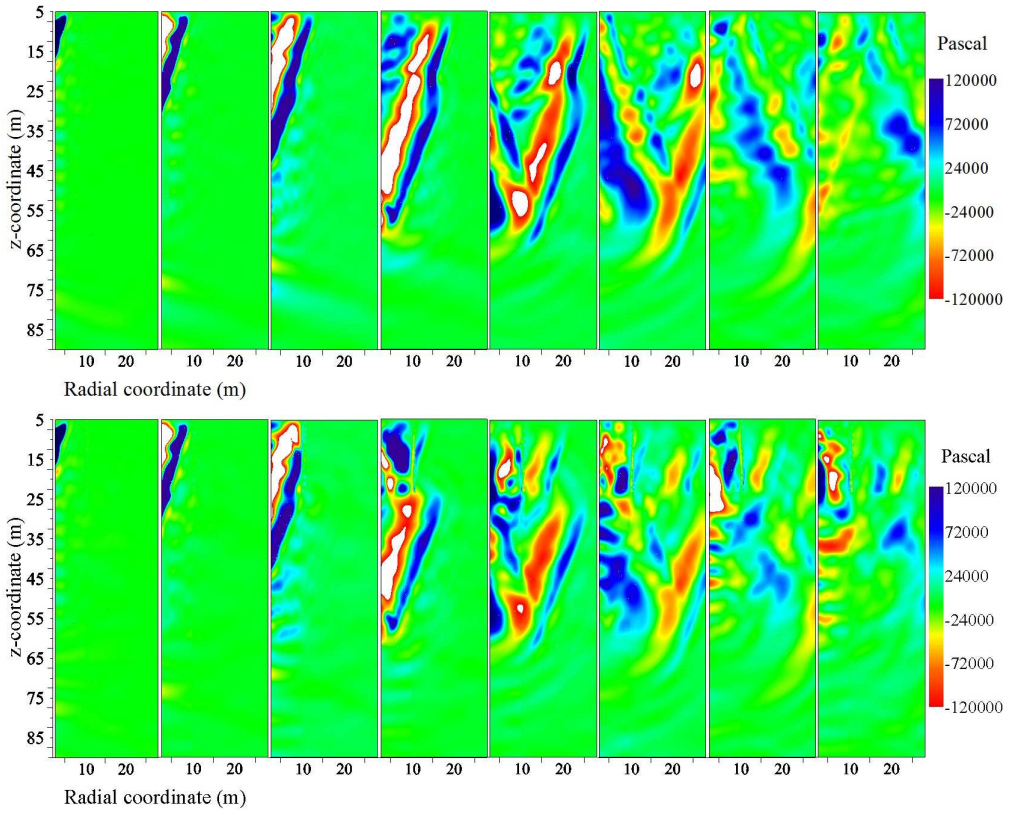


Figure 2: Pressure in the fluid and in the seabed for several moments in time after the hammer impact. The top and bottom figures correspond to the case without and with an air-bubble curtain, respectively. From left to right the time frame in milliseconds: $t = 9.6$; 12.0; 14.4; 19.2; 24.0; 28.8; 33.6; 38.4 [11].

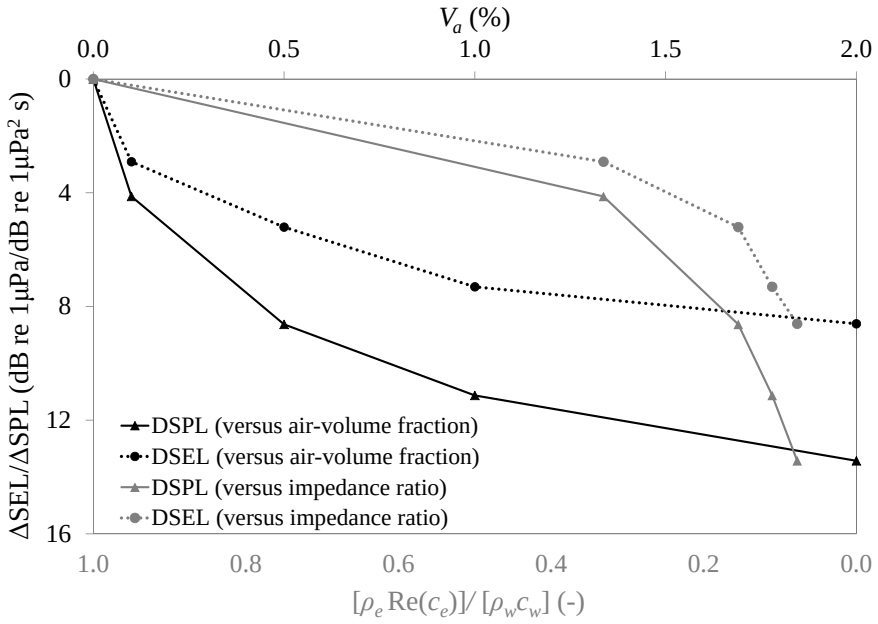


Figure 3: Difference in the SPL and the SEL for varying air-volume fraction (black colour) and for varying impedance contrast (grey colour) for a point positioned 2m above the seabed level at $r = 26.6$m from the pile axis [11]. SPL $= 20 \log_{10}(|p_{peak}|/10^{-6})$ and SEL $= 10 \log_{10}\left(1/t_0 \int_{t=t_5}^{t=t_{95}} p^2(t)/10^{-12} dt\right)$ with $t_0 = 1$s.

influential in comparison with the air-volume fraction described above [11] and are not discussed further in this paper.

### 3.2 Piles of small diameter

The results presented in the previous section cannot be generalised to piles of small diameter in which the sound radiation contains significant amount of energy in the vicinity of the resonance frequency and beyond. To illustrate this, the case in which $f > 1.2f_r$ is analysed. In [9], sound radiation from a foundation pile with a diameter of $0.9$m was examined in which considerable amount of energy was radiated around $2.5$kHz. Although such small piles are not encountered in the offshore wind industry, they are used in several other applications as, for example, in foundations of engineering structures in harbours or in the petroleum industry. For air-bubbles with radii up to $5$mm, radiation of sound at these frequencies would satisfy the inequality given above. Considering the relatively small fractional volume of air that is used in practical applications, one can note that for $f > 1.2f_r$ the ratio of the acoustic impedances tends to unity, i.e. $(\mathrm{Re}(\tilde{c}_e)\,\rho_e)\,/\,(c_w\,\rho_w) \to 1$, which actually implies that there will be hardly any reflection of the incident waves. In this case, one would need to rely primarily on the sound absorption within the bubbly layer in order to mitigate the noise. Additionally, when the excitation frequency is around the resonance frequency of the bubbles, i.e. $0.7f_r < f < 1.2f_r$, the bubbly medium is highly dispersive [15]. The wave speed reaches a minimum while the sound absorption maximises due to the resonating bubbles. Thus, it is to be expected that both the sound absorption within the bubbly layer and the acoustic impedance mismatch will contribute to the noise reduction.

## 4. Conclusions

In this study, a semi-analytical model is presented that can be used for the noise prediction with the use of an air-bubble curtain around a foundation pile. The model consists of the pile, the surrounding water-soil medium and the air-bubble curtain that is placed around the pile along the water column. The bubbly layer is described as a homogeneous medium with a frequency-dependent, complex-valued compressibility. The model is semi-analytical; due to adopted solution approach, different stages during the installation phase can be examined with minimum computational effort. A parametric study is performed in order to reveal the principal mechanisms that are responsible for the noise reduction. The distinction was made between piles of large and small diameter due to the considerable different spectrum of noise generated. In the case of practical applications related to the installation of large foundation piles only the lower end of the frequency spectrum is usually of interest. Thus, the creation of a dense layer of air-bubbles of relatively small radii seems to be advantageous over a less dense layer of bubbles of large radii yielding the same air-volume content. The dense and homogeneous *bubble cloud* will act as an *acoustic reflector* of the incident energy into the region formed between the pile and the air-bubble curtain. Provided that the energy spectrum of the radiated sound is located at relatively low frequencies, the radius of the bubbles is of secondary importance; what actually matters is the creation of a dense layer of uniformly distributed bubbles along the entire water column.

## REFERENCES

1. EWEA. European Wind Energy Association, The European offshore wind industry - key trends and statistics 2013, (2014).

2. David, J. A. Likely sensitivity of bottlenose dolphins to pile-driving noise, *Water and Environment Journal*, **20** (1), 48–54, (2006).

3. Madsen, P. T., Wahlberg, M., Tougaard, J., Lucke, K. and Tyack, P. Wind turbine underwater noise and marine mammals: implications of current knowledge and data needs, *Marine Ecology Progress Series*, **309**, 279–295, (2006).

4. Bailey, H., Senior, B., Simmons, D., Rusin, J., Picken, G. and Thompson, P. M. Assessing underwater noise levels during pile-driving at an offshore windfarm and its potential effects on marine mammals, *Marine Pollution Bulletin*, **60** (6), 888 – 897, (2010).

5. Erbe, C. International regulation of underwater noise, *Acoustics Australia*, **41** (1), 12 – 19, (2013).

6. Bellmann, M. A. Overview of existing noise mitigation systems for reducing pile-driving noise, *INTER-NOISE and NOISE-CON Congress and Conference Proceedings*, vol. 249, pp. 2544–2554, Institute of Noise Control Engineering, (2014).

7. Würsig, B., Greene, C. R. and Jefferson, T. A. Development of an air bubble curtain to reduce underwater noise of percussive piling, *Marine Environmental Research*, **49** (1), 79 – 93, (2000).

8. Göttsche, K. M., Juhl, P. M. and Steinhagen, U., *Numerical prediction of underwater noise reduction during offshore pile driving by a Small Bubble Curtain*, Proceedings of Internoise 2013: Noise Control for Quality of Life, Innsbruck, Austria. (2013).

9. Tsouvalas, A. and Metrikine, A. V. A semi-analytical model for the prediction of underwater noise from offshore pile driving, *Journal of Sound and Vibration*, **332** (13), 3232 – 3257, (2013).

10. Tsouvalas, A. and Metrikine, A. V. A three-dimensional vibroacoustic model for the prediction of underwater noise from offshore pile driving, *Journal of Sound and Vibration*, **333** (8), 2283 – 2311, (2014).

11. Tsouvalas, A. and Metrikine, A. V. Noise reduction by the application of an air-bubble curtain in offshore pile driving, *Journal of Sound and Vibration*, **371**, 150 – 170, (2016).

12. Kaplunov, Y. D., Kirillova, I. V. and Kossovich, L. Y. Asymptotic integration of the dynamic equations of the theory of elasticity for the case of thin shells, *Journal of Applied Mathematics and Mechanics*, **57** (1), 95–103, (1993).

13. Lippert, T. and von Estorff, O. The significance of parameter uncertainties for the prediction of offshore pile driving noise, *The Journal of the Acoustical Society of America*, **136** (5), 2463–2471, (2014).

14. Novarini, J. C., Keiffer, R. S. and Norton, G. V. A model for variations in the range and depth dependence of the sound speed and attenuation induced by bubble clouds under wind-driven sea surfaces, *IEEE Journal of Oceanic Engineering*, **23** (4), 423–438, (1998).

15. Hall, M. V. A comprehensive model of wind generated bubbles in the ocean and predictions of the effects on sound propagation at frequencies up to 40 kHz, *The Journal of the Acoustical Society of America*, **86** (3), 1103–1117, (1989).

16. Tsouvalas, A., van Dalen, K. N. and Metrikine, A. V. The significance of the evanescent spectrum in structure-waveguide interaction problems, *The Journal of the Acoustical Society of America*, **138** (4), 2574–2588, (2015).

17. Hamilton, E. L. Geoacoustic modeling of the sea floor, *The Journal of the Acoustical Society of America*, **68** (5), 1313–1340, (1980).